Mutagenesis of an active-site loop in tryptophan hydroxylase dramatically slows the formation of an early intermediate in catalysis

Bishnu P. Subedi, and Paul F. Fitzpatrick

J. Am. Chem. Soc., **Just Accepted Manuscript** • DOI: 10.1021/jacs.8b00936 • Publication Date (Web): 28 Mar 2018

Mutagenesis of an active-site loop in tryptophan hydroxylase dramatically slows the formation of an early intermediate in catalysis

Bishnu P. Subedi and Paul F. Fitzpatrick*

Department of Biochemistry and Structural Biology, University of Texas Health Science Center at San Antonio, San Antonio TX, 78229.

Solution studies of the aromatic amino acid hydroxylases are consistent with the $Fe^{IV}O$ intermediate not forming until both the amino acid and tetrahydropterin substrates have bound. Structural studies have shown that the positions of active-site loops differs significantly between the free enzyme and the enzyme-amino acid-tetrahydropterin complex. In tryptophan hydroxylase (TrpH) these mobile loops contain residues 124-134 and 365-371, with a key interaction involving Ile366. The I366N mutation in TrpH results in decreases of 1-2 orders of magnitude in the k_{cat} and k_{cat}/K_m values. Single turnover analyses establish that the limiting rate constant for turnover is product release for the wild-type enzyme but is formation of the first detectable intermediate **I** in catalysis in the mutant enzyme. The mutation does not alter the kinetics of NO binding to the ternary complex nor does it uncouple $Fe^{IV}O$ formation from amino acid hydroxylation. The effects on the k_{cat} value of wild-type TrpH of changing viscosity are consistent with rate-limiting product release. While the effect of viscosity on the k_{cat}/K_{O2} value is small, consistent with reversible oxygen binding, the effects on the k_{cat}/K_m values for tryptophan and the tetrahydropterin are large, with the latter value exceeding the expected limit and varying with the identity of the viscogen. In contrast, the kinetic parameters of I366N TrpH show small changes with viscosity. The results are consistent with binding of the amino acid and pterin substrate to form the ternary complex being directly coupled to closure of loops over the active site and formation of the reactive complex. The mutation destabilizes this initial event.

INTRODUCTION

The non-heme iron-containing enzyme tryptophan hydroxylase (TrpH) catalyzes the tetrahydropterin (PH_4)-dependent hydroxylation of tryptophan to 5-hydroxytryptophan (Scheme 1)[1] in the rate-limiting step in the biosynthesis of the neurotransmitter serotonin. The enzyme belongs to the family of tetrahydropterin-dependent aromatic amino acid hydroxylases (AAHs). The other members, phenylalanine hydroxylase (PheH) and tyrosine hydroxylase (TyrH), also selectively hydroxylate the aromatic side chains of their respective substrates. All three enzymes have similar active site geometries and catalytic mechanisms (Scheme 2) involving a ferryl-oxo ($Fe^{IV}O$) intermediate. [2-3] In this mechanism, the reactive $Fe^{IV}O$ undergoes an electrophilic attack by the aromatic ring of the amino acid substrate followed by a hydrogen shift to generate the hydroxylated product.[4-5] Recently, rapid-reaction studies of TrpH were used to determine the intrinsic rate constants in the reaction; this analysis allowed detection of a short-lived intermediate (**I**), formed after oxygen binds to the enzyme-substrate complex.[6] **I** reacts to yield the $Fe^{IV}O$ and 4a-hydroxypterin (PH_3OH).

Scheme 1. The TrpH reaction

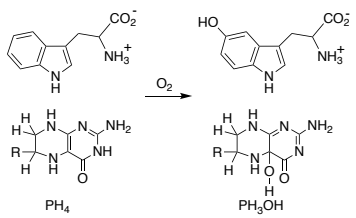

Kinetic studies of all three AAHs are consistent with binding of the tetrahydropterin and amino acid substrates to the enzyme before oxygen.[7-9] Crystallographic and spectroscopic studies have shown that formation of these ternary enzyme-amino acid-tetrahydropterin complexes is accompanied by a number of structural changes. In the crystal structures of the resting forms and enzyme-pterin binary complexes of all three enzymes, loops corresponding to residues 124-134 and 365-371 in TrpH1 are well-separated or absent (Figure 1).[10-12] In contrast, in the PheH enzyme-tetrahydropterin-phenyalanine[13] and the TrpH enzyme-imidazole-tryptophan[14] complexes, these loops have closed over the active site, with their central residues packing against one another. Although there is as yet no structure of TyrH with both substrates bound, fluorescence studies of that enzyme have shown that the loop corresponding to residues 124-134 in TrpH is less mobile in the enzyme-pterin binary complex and even less so in the ternary complex, suggesting that these loops also close over the active site in that enzyme when both substrates are bound.[15] Mutagenesis to valine of TyrH Asp425, which corresponds to TrpH Ile366, changes the relative specificity of the enzyme for phenylalanine versus tyrosine by five orders of magnitude, consistent with tight coupling between the structure of the loop containing that residue and the active site. Studies of PheH and TyrH have also shown that formation of the ternary complex is associated with changes in the active site structure. In ternary enzyme-pterin-substrate complexes of both enzymes, the glutamate that is one of the iron ligands has changed from being a monodentate ligand in the resting enzyme to bidentate coordination; the iron has changed from hexacoordinate, with three bound water molecules, to pentacoordinate as two water molecules are lost;

and the amino acid and pterin have shifted positions relative to the iron, so that they are better positioned for oxygen activation and hydroxylation.[13, 16-19] These structural changes upon formation of the ternary complex are associated with changes in the reactivity of the iron such that it reacts productively with oxygen to form the $Fe^{IV}O$,[17, 20] suggesting that reorganization of these surface loops controls the reactivity of the active site iron. We describe here the use of a combination of rapid-reaction and steady-state kinetic analyses with site-directed mutagenesis of Ile366 to probe the importance of loop interactions to catalysis in TrpH.

Scheme 2. Mechanism of TrpH

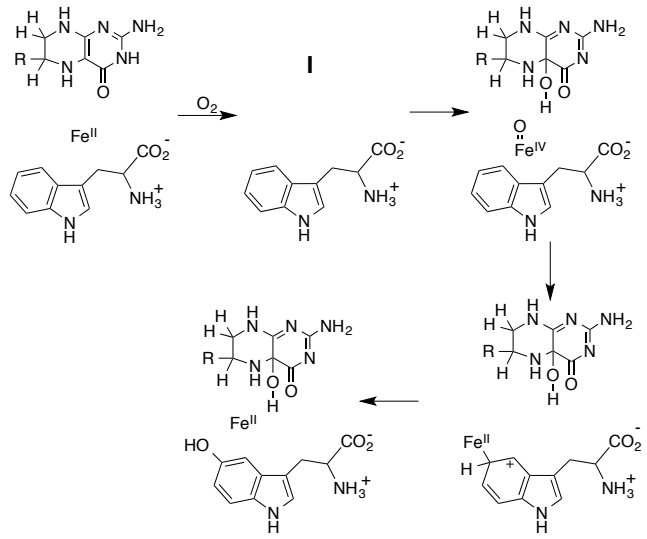

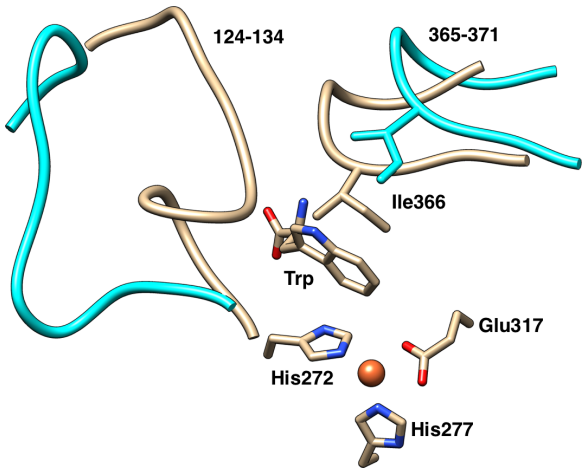

Figure 1. Movement of active-site loops in TrpH upon substrate binding [cyan: in the absence of ligands (PDB file 1MLW), gray: in the presence of tryptophan and imidazole (PDB file 3E2T)].

EXPERIMENTAL PROCEDURES

Materials. 6-Methyltetrahydropterin ($6MPH_4$) was purchased from Schircks Laboratories (Jona, Switzerland). Ampicillin and isopropyl ß-D-1-thiogalactopyranoside were from Research Products International Corp. (Mount Prospect, IL). Oligonucleotides were from Integrated DNA Technologies. Other chemicals/media were purchased from Sigma-Aldrich Co. LLC (St. Louis, MO) or ThermoFisher Scientific, Inc. (Waltham, MA). Site-directed mutagenesis of Ile366 to Asn in the plasmid pEWOHΔ101ΔH, which codes for expression of the catalytic domain of rabbit TrpH1, was performed using the QuikChange II protocol (Stratagene). The DNA sequence of the resulting vector was verified by sequencing (GenScript). Expression in *E. coli* and purification of the wild-type and mutant enzymes were carried out using previously described methods[21] but with 50 mM HEPES, pH 7.7, for buffers because of the much greater solubility of the enzyme at that pH. The lysis buffer was also changed to 50 mM HEPES, 50 mM ammonium sulfate, 10% glycerol, 1 mM tris(2-carboxyethyl) phosphine, 100 µg/mL lysozyme, 100 µg/mL phenylalanine, 10 µg/mL phenylmethanesulfonyl fluoride, 50 µg/mL EDTA, pH 7.7. The concentrations of the purified enzymes were determined using an ε_{280} value of 35,200 M^{-1} cm^{-1}.[22] The apoenzymes were prepared as previously described.[9]

Assays. The ratio of pterin oxidation to amino acid hydroxylation was measured by performing assays with a limited amount of pterin with the other substrates in excess. In a typical reaction, 5 µL of 10 mM $6MPH_4$ was added to 200 µM tryptophan, 10 µM enzyme, and 20 µM ferrous ammonium sulfate in 0.5 mL 50 mM HEPES, 50 mM ammonium sulfate, pH 7.7. The mixture was allowed to react for 20 min at room temperature and then 1 mL of 2 M HCl was added. The amount of hydroxylated tryptophan produced was determined by HPLC as previously described.[20]

Steady-state kinetic assays contained 0.25-1 µM wild-type or 0.5-3 µM mutant enzyme, 100 µg/mL catalase, 1 mM dithiothreitol, and 10 µM ferrous ammonium sulfate in 0.5 mL 50 mM HEPES, 50 mM ammonium sulfate, pH 7.7. The concentration of tryptophan in the reaction mixture was 200 µM when $6MPH_4$ was the varied substrate, and the concentration of $6MPH_4$ was 300 µM when tryptophan was the varied substrate. Each reaction was started by the addition of a small aliquot of 40 mM $6MPH_4$ in 1 mM HCl to the reaction mixture at 6 °C. The samples were allowed to react for 40 s (wild-type enzyme) or up to 120 s (I366N TrpH), and then 100 µL of the reaction mixture was added to 200 µL of 2 M HCl. The 5-hydroxytryptophan formed was determined by HPLC.[20] When glycerol, sucrose, or trehalose was added, the resulting viscosities were calculated using published values.[23] In all cases, the initial rates determined with multiple enzyme preparations were combined in the analyses to control for variations between enzyme preparations.

Rapid-reaction kinetics. Stopped-flow kinetic measurements were carried out using an Applied Photophysics SX-20 stopped-flow spectrophotometer (Leatherhead, UK). All data were collected at 6 °C. The instrument was made anaerobic by overnight incubation with glucose and glucose oxidase as previously described.[8] For a typical experiment, a solution of apoenzyme (~200 µM) and tryptophan (1 mM) in 10 mL of 50 mM HEPES, 50 mM ammonium sulfate, pH 7.7, was placed in a tonometer. Additionally, 8 µL ferrous ammonium sulfate (0.5 M) and 200 µL $6MPH_4$ (0.1 M) were placed in the side arm of the tonometer. The contents of the tonometer were made anaerobic using vacuum-argon cycles, and then they were mixed. Solutions containing different concentrations of oxygen were prepared by bubbling with mixtures of N_2 and O_2. Solutions of nitric oxide in anaerobic buffer were prepared from freshly prepared stock solutions of 6-(2-hydroxy-1-methyl-2-nitrosohydrazino)-*N*-methyl-1-hexanamine in 10 mM NaOH.[18]

Chemical-quench experiments were carried out using a BioLogic QFM-400 quench-flow instrument (Claix, France). In a typical experiment, an anaerobic mixture of 50 μM apoenzyme plus 100 μM ferrous ammonium sulfate and 2 mM $6MPH_4$ was reacted with 0.5 mM tryptophan in oxygen-saturated reaction buffer. The reaction was quenched at 0.04 to 20 s with 2 M HCl. The amount of 5-hydroxytryptophan formed at each time was determined by HPLC.

Data analysis. KaleidaGraph (Synergy) was used for fitting kinetic data. The steady-state kinetic parameters k_{cat}, K_m, and k_{cat}/K_m were determined using the Michaelis-Menten equation. The effects of viscosity on the k_{cat} and k_{cat}/K_m values were determined using eq 1;[6] here, Y^0 and Y are the k_{cat} or k_{cat}/K_m values in the absence and presence of added viscogen, η^0 and η are the viscosities of the buffer in the absence and presence of added viscogen, and n is the effect of viscosity on the kinetic parameter. Stopped flow traces with multiple phases were analyzed using eq 2, where i indicates the number of phases, k_{obsi} indicates the associated rate constant for the ith phase, A is the total absorbance change, A_0 is the absorbance at the start of the reaction, and A_i is the absorbance change associated with the ith phase. The rapid-quench data were analyzed using eq 3, where k_{burst} is the rate constant for the burst phase and k_{linear} is the subsequent linear rate. Global fitting of kinetic data and construction of mechanistic pathways were done using KinTek Explorer Pro 6.2 (KinTek Corp, Austin, TX).[24] KinTek's FitSpace Explorer[25] was used to determine confidence intervals.

$$Y = Y^0/(1 + n*(\eta/\eta^0 - 1)) \quad (1)$$

$$A_t = A_0 + \Sigma(\Delta A_i e^{-k_{obsi}t}) \quad (2)$$

$$([HO\text{-}trp]/[TrpH])_t = A_0(1 - e^{-k_{burst}t}) + k_{linear}t \quad (3)$$

RESULTS

Steady-State Kinetics. When the 365-371 and 124-134 loops close over the active sites of the AAHs, the central residue in the former packs against the aromatic side chain of a phenylalanine or tyrosine residue in the latter. That residue in the 364-371 loop in TrpH, Ile366, was initially mutated to aspartate to disrupt this hydrophobic interaction. However, the I366D enzyme was unstable and difficult to purify, precluding detailed studies of the effects of the mutation. Consequently, I366N TrpH was expressed; this enzyme proved to be suitable for characterization. The kinetic parameters of this mutant enzyme are given in Table 1 along with the values for the wild-type enzyme determined under identical conditions. The mutation results in a decrease of an order of magnitude in the k_{cat} and k_{cat}/K_{6MPH4} values, a 65-fold decrease in the k_{cat}/K_{Trp} value, and a 30-fold decrease in the k_{cat}/K_{O2} value.

Coupling of $6MPH_4$ oxidation to tryptophan hydroxylation. Mutagenesis of residues in the AAHs often results in the unproductive oxidation of the tetrahydropterin without hydroxylation of the amino acid substrate. To determine if the decreased activity of I366N TrpH was due in part to such uncoupling of the two partial reactions, the relative stoichiometry of tetrahydropterin oxidation and amino acid hydroxylation was determined. This was done by reacting the enzyme with 10 equivalents of $6MPH_4$ in the presence of excess tryptophan until all of the pterin had been oxidized and then measuring the amount of hydroxytryptophan that had been produced. This assay produced 80 ± 10 μM 5-hydroytryptophan from 100 μM $6MPH_4$. Therefore, the low activity of I366N TrpH is not due to unproductive pterin oxidation, so that the changes in the kinetic parameters of the mutant protein reflect changes in rate constants along the normal catalytic pathway.

Table 1. Steady-state kinetic parameters of wild-type and I366N TrpH[a]

kinetic parameter	wild-type TrpH	I366N TrpH
k_{cat} (s^{-1})[b]	0.27 ± 0.02	0.024 ± 0.003
K_{6MPH4} (μM)[b]	56 ± 9	42 ± 13
k_{cat}/K_{6MPH4} ($mM^{-1}s^{-1}$)[b]	4.7 ± 0.5	0.58 ± 0.14
K_{Trp} (μM)[c]	7.3 ± 2.5	99 ± 31
k_{cat}/K_{Trp} ($mM^{-1}s^{-1}$)[c]	21 ± 6	0.32 ± 0.06
K_{O2} (μM)[d]	33 ± 3	210 ± 91
k_{cat}/K_{O2} ($mM^{-1}s^{-1}$)[d]	6.6 ± 0.6	0.21 ± 0.06

[a]Assay conditions: 0.25-3 μM TrpH, 100 μg/mL catalase, 1 mM dithiothreitol, 10 μM ferrous ammonium sulfate, 50 mM HEPES, 50 mM ammonium sulfate, pH 7.7, 6 °C.

[b]200 μM Trp, 10-300 μM $6MPH_4$, 390 μM O_2

[c]300 μM $6MPH_4$, 3-200 μM Trp, 390 μM O_2

[d]200 μM Trp, $6MPH_4$, 20-300 μM O_2

Viscosity effect on steady-state kinetic parameters. k_{cat} and k_{cat}/K_m values are combinations of rates constants for catalytic steps and for the diffusion of substrates into or products out of the active site. To determine to what extent diffusion limits substrate binding (k_{cat}/K_m) and product release (k_{cat}) for the wild-type and mutant enzymes, the effects of increasing the viscosity of the solvent on the steady-state kinetics were determined. Glycerol, sucrose, and trehalose were used as viscogens in analyses of the k_{cat}, k_{cat}/K_{6MPH4}, and k_{cat}/K_{Trp} values, while only sucrose and trehalose were used in the analysis of the k_{cat}/K_{O2} values due to the much smaller effects in that case. The effects on the k_{cat} and k_{cat}/K_{Trp} values were independent of the viscogen, so that the results were combined in the analyses of those kinetic parameters. However, glycerol consistently had a larger effect than sucrose and trehalose on the k_{cat}/K_{6MPH4} value, so that the effects of glycerol were analyzed separately in that case.

The extent to which diffusion limits a kinetic parameter is given by the value of n in eq 1. A value of zero indicates that diffusive steps are much faster than one or more first-order steps, while a value of one indicates that a kinetic parameter only reflects substrate binding or product release.[26-27] The data for wild-type and I366N TrpH are shown in Figure 2 and Table 2. For wild-type TrpH, the k_{cat} and k_{cat}/K_{Trp} values have n values of unity. This is consistent with product release fully limiting the former and substrate diffusion into the active site fully limiting the latter. In contrast the effect of viscosity on the k_{cat}/K_{O2} value is small, suggesting that O_2 binding is not diffusion-limited. The effects of viscosity on the k_{cat}/K_{6MPH4} are anomalous. In addition to the effect depending on the identity of the viscogen, the effects are substantially greater than the expected limiting value of one.

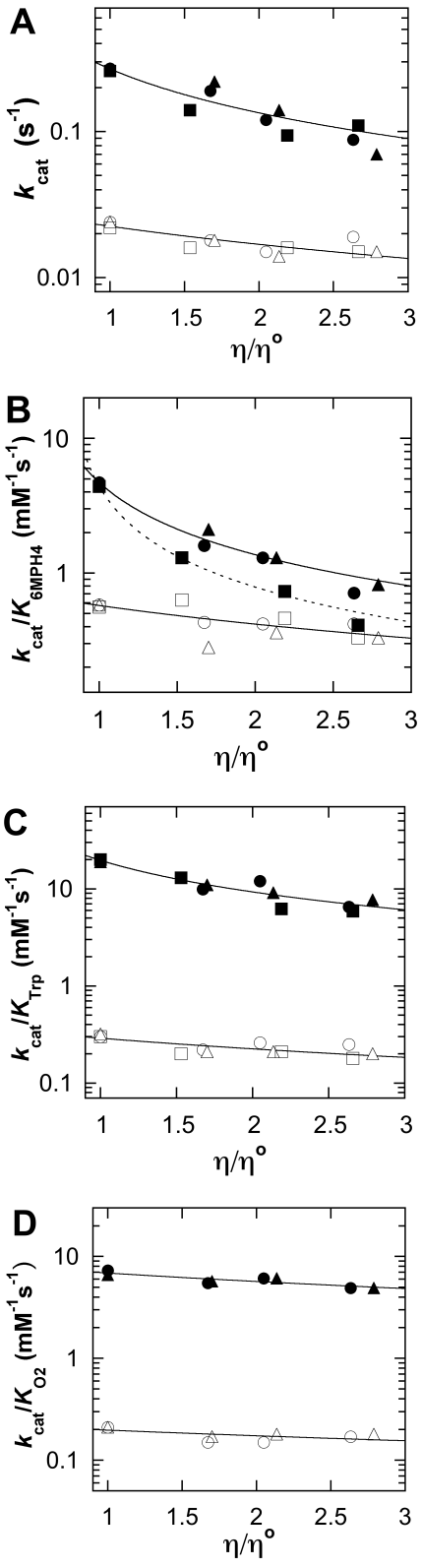

Figure 2. Effect of solvent viscosity on the steady-state kinetic parameters for wild-type (filled symbols) and I366N (empty symbols) TrpH using sucrose (circles), trehalose (triangles) or glycerol (squares) as the viscogen. The lines are from fits with eq 2; in B, the dotted line is for a fit of the glycerol data for the wild-type enzyme alone. Conditions: 50 mM HEPES, 50 mM ammonium sulfate, pH 7.7, 0-30 % sucrose, trehalose, or glycerol, 6 °C.

Table 2. Viscosity effects on the steady-state kinetic parameters of wild-type and I366N TrpH*

Enzyme	k_{cat}	k_{cat}/K_{6MPH4}	k_{cat}/K_{Trp}	k_{cat}/K_{O2}
Wild-type TrpH	1.0 ± 0.2[a]	2.4 ± 0.2[b] 4.6 ± 0.3[c]	1.1 ± 0.1[a]	0.21 ± 0.06[b]
I366N TrpH	0.33 ± 0.08	0.37 ± 0.13	0.29 ± 0.10	0.13 ± 0.08[b]

*The values are based on fitting the data in Figure 2 to eq 1, to obtain n, the viscosity effect. The conditions are as described for Table 1 plus 0-30 % sucrose, trehalose or glycerol.

[a]Based on the combined data with sucrose, trehalose, and glycerol as viscogens.

[b]Based on the combined data with sucrose and trehalose as viscogens.

[c]Based on the data with glycerol as the viscogen.

In contrast to the results with the wild-type enzyme, the steady-state kinetic parameters for I366N TrpH are relatively insensitive to viscosity. This suggests that the mutation has decreased the rate constant(s) for one or more first-order steps significantly more than those for substrate binding and product release.

Nitric oxide binding kinetics. The reaction of nitric oxide with the active-site Fe(II) has previously been used as a model for the reaction of oxygen with the AAHs[18-19, 28] and other non-heme iron enzymes.[29] Consequently, the kinetics of the formation of the nitrosyl complex by the TrpH/6MPH$_4$/tryptophan complex were examined for the wild-type and mutant. Mixing of the ternary complex with 0.5 mM nitric oxide resulted in rapid increase in the near-UV absorbance for both wild-type and mutant TrpH (results not shown). At 420 nm, the wavelength at which the absorbance change was greatest, the reaction was clearly biphasic for both enzymes (Figure 3). The reactions of the wild-type and mutant enzymes showed comparable rate constants for nitric oxide binding (k_{obs1} = 79 ± 1 versus 71 ± 1 s^{-1} and k_{obs2} = 5.2 ± 0.2 versus 5.2 ± 0.3 s^{-1} respectively). Thus, the mutation does not alter the reactivity of the iron center with NO.

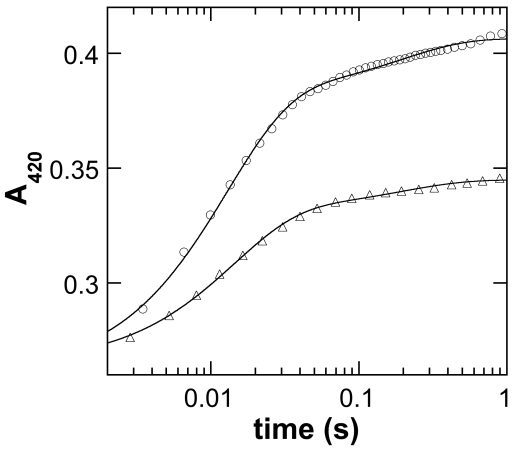

Figure 3. Absorbance changes during the anaerobic reaction of 0.5 mM nitric oxide with the TrpH-6-MPH$_4$-tryptophan complex (100 μM) for wild-type (o) and I366N (Δ) TrpH. The lines are from fits using eq 3 with two phases. Conditions: 50 mM HEPES, 50 mM ammonium sulfate, pH 7.7, 6 °C.

Single turnover kinetics To measure intrinsic rate constants for individual steps during enzyme catalysis, enzyme-substrate complexes of both the wild-type and the mutant enzyme were mixed with solutions of buffer containing 200, 400, or 600 μM oxygen. Reactions were followed at 246, 336, and 410 nm. Formation of the 4a-hydroxypterin product, which occurs in the same step as formation of the $Fe^{IV}O$ (Scheme 2) is associated with an increase in absorbance at 248 nm and a decrease at 336 nm. A transient intermediate that precedes the hydroxypterin has previously been detected at 410 nm.[20] Product release also results in increases at 248, 336, and 410 nm. Representative traces are shown in Figure 4. The wild-type enzyme clearly shows an increase in absorbance at 246 nm and a small decrease at 336 nm over the first 300 ms, while the mutant enzyme shows no changes at these wavelengths over the first second. More critically, the formation and decay of an intermediate is clearly seen at ~100 ms with the wild-type enzyme at 410 nm, but there is no change at that wavelength with I366N TrpH over the first second. At longer times both enzymes show absorbance increases, but this occurs more slowly with the mutant protein.

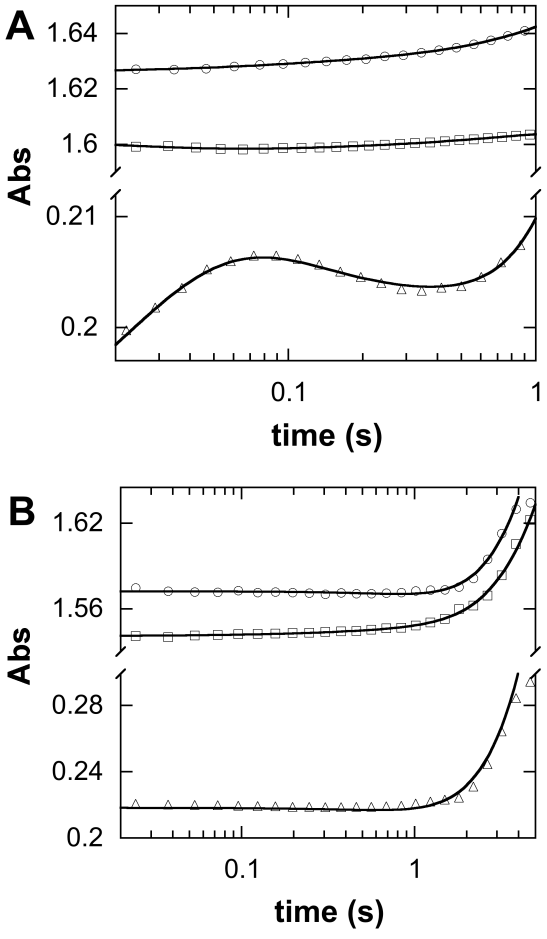

Figure 4. Absorbance changes at 246 (○), 336 (□), and 410 (Δ) nm during the reaction of 100 μM wild-type (A) or I366N (B) TrpH with 500 μM tryptophan, 1 mM $6MPH_4$, and 400 μM oxygen. The lines are from the kinetic mechanism in Scheme 3 and the corresponding kinetic parameters in Table 3. Conditions as described for Figure 3.

Chemical-quench methods were used to directly measure the effect of the mutation on the kinetics of formation of 5-hydroxytryptophan. An anaerobic solution of enzyme plus an excess of $6MPH_4$ was rapidly mixed with excess tryptophan in oxygen-saturated buffer. The samples were acid quenched at various times and the product was analyzed by HPLC. Figure 5 shows the amount of product formation with time for both enzymes. The wild-type data show a burst of product formation and consequently were fit to eq 3 to obtain a burst amplitude of 0.29 ± 0.03, a k_{burst} value of 9.6 ± 2.9 s^{-1} and a k_{linear} value of 0.18 ± 0.01 s^{-1}. In contrast, the data for the mutant enzyme were better fit with a straight line to give a k_{linear} value of 0.028 ± 0.001 s^{-1}.

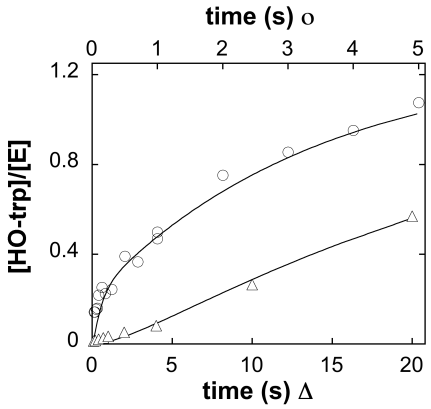

Figure 5. Chemical-quench analyses of tryptophan hydroxylation by wild-type (o) or I366N (Δ) TrpH (50 μM) with 1 mM $6MPH_4$, 0.5 mM tryptophan, and 0.9 mM oxygen. The lines are from the kinetic mechanism in Scheme 3 and the corresponding kinetic parameters in Table 3. Conditions as described for Figure 3.

Global data analysis and kinetic mechanism. The stopped-flow results at all three wavelengths and oxygen concentrations and the rapid-quench results were combined to derive a kinetic mechanism for the reaction of the TrpH-tryptophan-$6MPH_4$ complex with oxygen. This was done using the program Global Kinetic Explorer,[24] which uses numerical intergration to fit time-course data to a kinetic model. A major advantage of this program is that it allows one to use a single kinetic model to simultaneously fit multiple sets of kinetic data. The quality of the fitting to each model was determined based on visual comparison of the predicted results with the data and on the X^2 value, which more quantitatively describes how well the model matches the data. While this analysis also generates error estimates for the individual rate constants, we instead used FitSpace Explorer[25] to determine the confidence intervals for the rate constants. This program determines confidence intervals by incrementally changing the value of an individual rate constant and then refitting the entire data set, allowing all of the other rate constants to vary. This process is continued iteratively until the X^2 value surpasses a preset maximum. We used a X^2 threshold of 0.88; this means that the X^2 value for the perturbed model was 1/0.88 times (or ~14% greater than) the X^2 value for the initial optimized fit. A change in the X^2 value of this magnitude is clearly detectable in plots overlaying the results of the fitting with the actual data. (The confidence intervals generated in this fashion are always greater than the errors calculated from the initial optimized fitting.) This approach is particularly good at detecting when a kinetic parameter is poorly determined, in that it can be varied over a large range without significantly degrading the fit, and when the values for two rate constants are coupled

and thus cannot be independently determined. Among the output of the FitSpace analyses are two-dimensional plots of the range over which two different rate constants can be varied without exceeding the X^2 threshold. These plots are shown in Figures S1 and S2 for the best fits for the wild-type and mutant enzyme and clearly show that all of the rate constants in the final model are well-constrained.

We previously used this approach to analyze the kinetics of wild-type TrpH.[20] Because the present results were obtained under slightly different conditions than in that study (pH 7.7 instead of pH 7.0 due to greatly improved stability of the enzyme) we first analyzed the data for wild-type TrpH. Visual inspection of the data at 410 nm in Figure 4 shows that there is a minimum of three phases; the data in Figure 5 require a separate step for product release. In addition, the observed rate constant for the initial phase of the absorbance changes was oxygen-dependent, so that an oxygen binding step is involved. Reversible binding of oxygen was previously described for wild-type TrpH.[20] These considerations yield the minimal mechanism of Scheme 3, which includes reversible oxygen binding, formation and decay of the 410 nm intermediate **I**, product release, and the nonenzymatic dehydration of the hydroxypterin product. The present data for the wild-type enzyme were well-fit with this kinetic mechanism (Figures 4A, 5, and S1). The rate constant for the nonenzymatic dehydration of the hydroxypterin to the quinonoid dihydropterin (qPH_2) was previously determined, so it was not varied in our analyses.[6] Addition of a step in which the decay of intermediate **I** to the $Fe^{IV}O$ plus the hydroxypterin is followed by hydroxylation of tryptophan as in Scheme 2 and described previously at pH 7.0 did not result in an improved fit of the data based on the lack of a decrease in the X^2 value (results not shown). The kinetic parameters resulting from the global analysis of the data for wild-type TrpH are given in Table 3. The mechanism of Scheme 3 was then used to analyze the data for I366N TrpH, providing a good fit of the data, with all of the kinetic parameters well-defined (Figures 4B, 5, and S2). These kinetic parameters are also given in Table 3.

For wild-type TrpH, the rate constants in Table 3 identify product release from the enzyme as the slowest step. In the case of I366N TrpH, the slow step is the formation of the early intermediate **I**, for which the rate constant k_2 has decreased by three orders of magnitude

Table 3. Rate constants for the reaction of the TrpH-pterin-tryptophan complex with oxygen.

Kinetic parameter	wild-type TrpH	I366N
K_{O2} (μM)	78 (70-83)[a]	4.1 (3.7-4.4)
k_2 (s^{-1})	68 (65-73)	0.031 (0.027-0.036)
k_3 (s^{-1})	7.9 (7.1-9.0)	1.5 (0.98-3.0)
k_4 (s^{-1})	0.29 (0.27-0.31)	0.38 (0.29-0.53)
k_5 (s^{-1})	0.024[b]	0.024

[a]Confidence intervals based on a X^2 threshold of 0.88.

[b]From Eser et al.[20]

Scheme 3. Kinetic Mechanism for TrpH

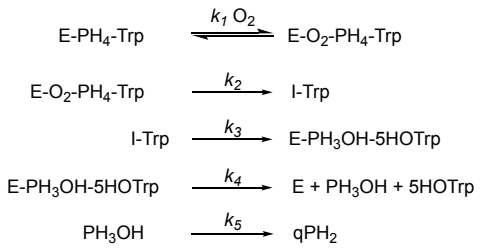

DISCUSSION

Monooxygenation reactions necessarily involve highly reactive oxidative intermediates whose reactivity must be tightly controlled to avoid deleterious or unproductive side reactions. A general strategy adopted by enzymes catalyzing such reactions is to prevent the formation of the oxidizing intermediate until the substrate has been bound. For example, in the case of the cytochrome P450 family of enzymes, the transfer of the second electron required for formation of the $Fe^{IV}O$-heme radical cation does not occur until the substrate is bound.[30] With non-heme iron alpha-ketoglutarate-dependent enzymes, binding of the substrate and reductant results in a change in the iron ligands that opens up a site for the productive binding of oxygen.[31] In most flavoprotein hydroxylases, the flavin is reduced very slowly in the absence of substrate, preventing the unwanted formation of the flavin hydroperoxide.[32] These changes in the reactivity of the cofactors upon substrate binding necessarily involve changes in protein structure that are poorly understood. [33-35]

The results from studies of all three AAHs to date have established that the $Fe^{IV}O$ hydroxylating intermediate similarly does not form until the amino acid and pterin substrates are bound. Crystallographic and spectroscopic studies of these enzymes have shown that the ternary enzyme-amino acid-pterin complex differs from the free enzyme in the position of active-site loops and the ligand environment of the iron.[13-14, 16-17] These results suggest that closure of active site loops over the active site is tightly coupled to initiation of catalysis. The present results provide support for such a proposal.

A key interaction between the 124-134 and 365-371 loops in the ternary complexes of the AAHs is between the residue equivalent to TrpH Ile366 and an aromatic residue in the opposite loop (Tyr125 in TrpH). The residue equivalent to TrpH Ile366 shows a unique pattern of conservation in the AAHs: this residue is isoleucine in TrpH, leucine in PheH and aspartate in TyrH.[36] In both PheH and TyrH this residue plays a key role in determining the substrate specificity of the enzyme, consistent with a direct link between the positioning of the surface loops and active site structure.[36-37] The I366N mutation was designed to disrupt this critical interaction to probe its importance in catalysis.

Mutagenesis of Ile366 to asparagine results in a significant decrease in the activity of the enzyme, with the k_{cat} and k_{cat}/K_m values of the enzyme decreasing 1-2 orders of magnitude from the wild-type values. These changes actually underestimate the effects of the mutation on individual rate constants. For wild-type TrpH, the k_{cat} value is effectively the rate constant for product release rather than reflecting rate constants for chemical steps. Qualitatively, the effect of rate-limiting product release is seen in the burst of hydroxylated amino acid formed in the first turnover (Figure 5). Quantitatively, the value of k_4, the

rate constant for product release in Table 3, matches the k_{cat} value and is ~30-fold slower than k_3, the next slowest step. The conclusion that product release is rate-limiting for the wild-type enzyme is also supported by the effect of solvent viscosity on the k_{cat} value. Irrespective of the viscogen used, the complete sensitivity of the k_{cat} value to viscosity is consistent with a diffusive step such as product release being >10-fold slower than preceding first-order steps. Based on the single-turnover analyses (Table 3), the largest effect of the I366N mutation is on the rate constant for formation of the early intermediate **I**, k_2. The value of this rate constant has decreased by 3 orders of magnitude, such that the formation of **I** is rate-limiting for turnover of the mutant enzyme. As a result, in the mutant enzyme this intermediate decays much more quickly than it forms, so that it is thus undetectable at 410 nm (Figure 4A), there is no longer a burst of product formation (Figure 5), and the k_{cat} value is significantly less sensitive to the solvent viscosity.

While the combination of steady-state and rapid-kinetic analyses thus provide a consistent picture of the effect of the I366N mutation on catalysis and the reason for the decreased k_{cat} value in the mutant protein, the effects on the k_{cat}/K_m values are more complex. k_{cat}/K_m values are combinations of binding steps and subsequent steps through the first irreversible step. The single-turnover results presented here and previous studies of all three AAHs are consistent with oxygen binding to the enzyme-amino acid-pterin complex reversibly; in such cases no viscosity effect is expected. In the TyrH-catalyzed reaction the first irreversible step after oxygen binding involves a change in the bond order to oxygen due to single-electron transfer involving the iron and/or pterin,[17, 38] and that is likely the case with TrpH. Electron transfer is also not expected to be viscosity-sensitive. Thus, the small effect of viscosity on the k_{cat}/K_{O2} value is fully consistent with oxygen binding being reversible and the first subsequent irreversible step involving single-electron transfer.

Previous steady-state kinetic analyses of TrpH suggest that the order of binding of the pterin and the amino acid is random, in that the k_{cat}/K_m value for the pterin differs several-fold when phenylalanine is the substrate rather than tryptophan, and the k_{cat}/K_m value for the amino acid similarly changes several-fold when tetrahydrobiopterin is used in place of 6-MPH_4.[22] In such a situation, the measured k_{cat}/K_{Trp} value will reflect binding of the amino acid to the enzyme-pterin binary complex, while the measured k_{cat}/K_{MPH4} value will reflect binding to the enzyme-amino acid complex. The effect of viscosity on the k_{cat}/K_{Trp} value is consistent with diffusion of the amino acid into the active site being followed by a rapid irreversible step, so that the k_{cat}/K_{Trp} value directly reflects the rate constant for productive entry of the amino acid into the active site. Since the value of this parameter is several orders of magnitude less than the diffusion limit, it is likely that this step is more complex than a simple encounter.

The magnitude of the effect of viscosity on the k_{cat}/K_{6MPH4} value is both larger than expected for a simple diffusive process and dependent on the identity of the viscogen. These results are not consistent with this kinetic parameter reflecting simply the rate constant for diffusion of the pterin into the enzyme active site. Instead, the effects of viscosity on the k_{cat}/K_{6MPH4} value suggests that there is a direct interaction of the viscogens with the protein.[39] While there do not appear to have been previous reports of viscosity effects of this magnitude on enzyme kinetics, there have been reports of increases in enzyme activity in the presence of viscogens.[40-41] These effects were attributed to stabilization of a more active conformation of the enzyme. Stabilization of a less-reactive form of TrpH by viscogens would be expected to affect other kinetic parameters, especially the k_{cat} value, since the result would be a lower concentration of the active form of the protein. However, as noted above, the effects of viscosity on the k_{cat} value for TrpH are fully consistent with rate-limiting product release. In addition, a similar stabilization of a less-reactive form of the protein would be expected for the I366N enzyme, while this enzyme is instead much less sensitive to viscosity. A more likely explanation for the effect of the viscosity on the k_{cat}/K_{6MPH4} is that the effect is kinetic, in that the effect is on the rate constant for binding of the pterin to the enzyme-amino acid complex. As is the case with the k_{cat}/K_{Trp} value, this step must be followed by a much faster and effectively irreversible step. The k_{cat}/K_{6MPH4} value of 5000 $M^{-1}s^{-1}$ is far below the diffusion limit, suggesting that this parameter does not simply reflect diffusion of the pterin into the active site. A direct coupling to pterin binding of closure of the 124-134 and 365-371 loops over the active site and the accompanying rearrangement to the oxygen-reactive form provides a structural rationale for the viscosity effect if the viscogen slows these structural changes. The effect of viscosity on the k_{cat}/K_{Trp} value may have a similar structural basis, given the relatively low value of this kinetic parameter and the large effect of viscosity.

An alternate explanation for the large viscosity effects is that the viscogens alter the equilibrium for the active closed form versus the unreactive open form of the enzyme. Such a model is difficult to reconcile with the properties of the mutant enzyme. It is not obvious why the mutant protein would not exhibit a similar change in the equilibrium constant and thus a similar viscosity effect. If the mutation instead resulted in a decreased stability of the closed form of the enzyme by increasing the rate constant for loop opening, the formation of the closed form of the enzyme would be closer to equilibrium and thus less sensitive to viscosity. This hypothesis also provides an explanation for the lack of a change in the kinetics of NO binding. In this experiment the ternary enzyme-tryptophan-pterin complex is preformed, so that a decrease in the rate constant for its formation will not be reflected in the kinetics. The lack of an effect on NO binding is consistent with the mutation not affecting steps in the chemical mechanism. Such a conclusion is supported by the finding that the mutation does not uncouple the formation of the $Fe^{IV}O$ and hydroxylation of the amino acid, in contrast to a number of other active site mutations.

The present results thus support a model in which the reactivity of the iron center in TrpH and the other AAHs is tightly controlled by the protein structure. Substrate binding to form the ternary enzyme-amino acid-pterin complex is required to form a productive oxygen-reactive species and is directly coupled to the movement of active-site loops seen in crystal structures.

ASSOCIATED CONTENT

Supporting Information

The Supporting Information is available free of charge on the ACS Publications website.

Figures S1-2. (PDF). FitSpace contour plots of single turnover analyses for wild-type and I366N TrpH

AUTHOR INFORMATION

Corresponding Author

*Phone (210) 567-8264. E-mail fitzpatrickp@uthscsa.edu.

Author Contributions

The manuscript was written through contributions of both authors.

Acknowledgments

This work was supported in party by grants from the National Science Foundation (CHE-1404129) and The Welch Foundation (AQ-1245).

ABBREVIATIONS

TrpH, tryptophan hydroxylase; TyrH, tyrosine hydroxylase; PheH, phenylalanine hydroxylase; $6MPH_4$, 6-methyltetrahydropterin.

REFERENCES

1. Fitzpatrick, P. F., Tetrahydropterin-dependent amino acid hydroxylases. *Ann. Rev. Biochem.* **1999,** *68*, 355-381.
2. Fitzpatrick, P. F., Mechanism of aromatic amino acid hydroxylation. *Biochemistry* **2003,** *42*, 14083-14091.
3. Roberts, K. M.; Fitzpatrick, P. F., Mechanisms of tryptophan and tyrosine hydroxylase. *IUBMB Life* **2013,** *65* (4), 350-357.
4. Hillas, P. J.; Fitzpatrick, P. F., A mechanism for hydroxylation by tyrosine hydroxylase based on partitioning of substituted phenylalanines. *Biochemistry* **1996,** *35*, 6969-6975.
5. Moran, G. R.; Derecskei-Kovacs, A.; Hillas, P. J.; Fitzpatrick, P. F., On the catalytic mechanism of tryptophan hydroxylase. *J. Am. Chem. Soc.* **2000,** *122* (19), 4535-4541.
6. Eser, B. E.; Fitzpatrick, P. F., Measurement of intrinsic rate constants in the tyrosine hydroxylase reaction. *Biochemistry* **2010,** *49* (3), 645-652.
7. Fitzpatrick, P. F., The steady state kinetic mechanism of rat tyrosine hydroxylase. *Biochemistry* **1991,** *30*, 3658-3662.
8. Roberts, K. M.; Pavon, J. A.; Fitzpatrick, P. F., Kinetic mechanism of phenylalanine hydroxylase: intrinsic binding and rate constants from single-turnover experiments. *Biochemistry* **2013,** *52* (6), 1062-1073.
9. Subedi, B. P.; Fitzpatrick, P. F., Kinetic mechanism and intrinsic rate constants for the reaction of a bacterial phenylalanine hydroxylase. *Biochemistry* **2016,** *55* (49), 6848-6857.
10. Goodwill, K. E.; Sabatier, C.; Marks, C.; Raag, R.; Fitzpatrick, P. F.; Stevens, R. C., Crystal structure of tyrosine hydroxylase at 2.3 Å and its implications for inherited neurodegenerative diseases. *Nat. Struct. Biol.* **1997,** *4*, 578-585.
11. Andersen, O. A.; Flatmark, T.; Hough, E., High resolution crystal structures of the catalytic domain of human phenylalanine hydroxylase in its catalytically active Fe(II) form and binary complex with tetrahydrobiopterin. *J. Mol. Biol.* **2001,** *314*, 279-291.
12. Wang, L.; Erlandsen, H.; Haavik, J.; Knappskog, P. M.; Stevens, R. C., Three-dimensional structure of human tryptophan hydroxylase and its implications for the biosynthesis of the neurotransmitters serotonin and melatonin. *Biochemistry* **2002,** *41* (42), 12569-12574.
13. Andersen, O. A.; Stokka, A. J.; Flatmark, T.; Hough, E., 2.0 Å Resolution crystal structures of the ternary complexes of human phenylalanine hydroxylase catalytic domain with tetrahydrobiopterin and 3-(2-thienyl)-L-alanine or L-norleucine: substrate specificity and molecular motions related to substrate binding. *J. Mol. Biol.* **2003,** *333* (4), 747-757.
14. Windahl, M. S.; Petersen, C. R.; Christensen, H. E.; Harris, P., Crystal structure of tryptophan hydroxylase with bound amino acid substrate. *Biochemistry* **2008,** *47* (46), 12087-12094.
15. Sura, G. R.; Lasagna, M.; Gawandi, V.; Reinhart, G. D.; Fitzpatrick, P. F., Effects of ligands on the mobility of an active-site loop in tyrosine hydroxylase as monitored by fluorescence anisotropy. *Biochemistry* **2006,** *45* (31), 9632-9638.
16. Wasinger, E. C.; Mitić, N.; Hedman, B.; Caradonna, J.; Solomon, E. I.; Hodgson, K. O., X-Ray absorption spectroscopic investigation of the resting ferrous and cosubstrate-bound active sites of phenylalanine hydroxylase. *Biochemistry* **2002,** *41* (20), 6211-6217.
17. Chow, M. S.; Eser, B. E.; Wilson, S. A.; Hodgson, K. O.; Hedman, B.; Fitzpatrick, P. F.; Solomon, E. I., Spectroscopy and kinetics of wild-type and mutant tyrosine hydroxylase: Mechanistic insight into O_2 activation. *J. Am. Chem. Soc.* **2009,** *131*, 7685-7698
18. Krzyaniak, M. D.; Eser, B. E.; Ellis, H. R.; Fitzpatrick, P. F.; McCracken, J., A pulsed EPR study of amino acid and tetrahydropterin binding in a tyrosine hydroxylase nitric oxide complex: Evidence for substrate rearrangements in formation of the oxygen-reactive complex. *Biochemistry* **2013,** *52* (47), 8430-8441.
19. McCracken, J.; Eser, B. E.; Mannikko, D.; Krzyaniak, M. D.; Fitzpatrick, P. F., HYSCORE Analysis of the effects of substrates on coordination of water to the active site iron in tyrosine hydroxylase. *Biochemistry* **2015,** *54*, 3759-3771.
20. Pavon, J. A.; Eser, B. E.; Huynh, M. T.; Fitzpatrick, P. F., Single turnover kinetics of tryptophan hydroxylase: Evidence for a new intermediate in the reaction of the aromatic amino acid hydroxylases. *Biochemistry* **2010,** *49*, 7563–7571.
21. Pavon, J. A.; Fitzpatrick, P. F., Insights into the catalytic mechanisms of phenylalanine and tryptophan hydroxylase from kinetic isotope effects on aromatic hydroxylation. *Biochemistry* **2006,** *45*, 11030-11037.
22. Moran, G. R.; Daubner, S. C.; Fitzpatrick, P. F., Expression and characterization of the catalytic core of tryptophan hydroxylase. *J. Biol. Chem.* **1998,** *273* (20), 12259-12266.
23. Rampp, M.; Buttersack, C.; Ludemann, H. D., c,T-dependence of the viscosity and the self-diffusion coefficients in some aqueous carbohydrate solutions. *Carbohydr. Res.* **2000,** *328*, 561-572.
24. Johnson, K. A.; Simpson, Z. B.; Blom, T., Global Kinetic Explorer: A new computer program for dynamic simulation and fitting of kinetic data. *Anal. Biochem.* **2009,** *387* (1), 20-29.
25. Johnson, K. A.; Simpson, Z. B.; Blom, T., FitSpace Explorer: An algorithm to evaluate multidimensional parameter space in fitting kinetic data. *Anal. Biochem.* **2009,** *387* (1), 30-41.
26. Nakatani, H.; Dunford, H. B., Meaning of diffusion-controlled association rate constants in enzymology. *J. Phys. Chem.* **1979,** *83* (20), 2662-2665.
27. Brouwer, A. C.; Kirsch, J. F., Investigation of diffusion-limited rates of chymotrypsin reactions by viscosity variation. *Biochemistry* **1982,** *21*, 1302-1307.
28. Han, A. Y.; Lee, A. Q.; Abu-Omar, M. M., EPR and UV-Vis studies of the nitric oxide adducts of bacterial phenylalanine hydroxylase: effects of cofactor and substrate on the iron environment. *Inorg. Chem.* **2006,** *45* (10), 4277-4283.
29. Gaffney, B. J., EPR of Mononuclear Non-Heme Iron Proteins. *Biol Magn Reson* **2009,** *28*, 233-268.
30. Ortiz de Montellano, P. R., Hydrocarbon Hydroxylation by Cytochrome P450 Enzymes. *Chem. Rev.* **2009,** *110* (2), 932-948.
31. Solomon, E. I.; Light, K. M.; Liu, L. V.; Srnec, M.; Wong, S. D., Geometric and electronic structure contributions to function in non-heme iron enzymes. *Acc. Chem. Res.* **2013,** *46* (11), 2725-39.
32. Ortiz-Maldonado, M.; Entsch, B.; Ballou, D. P., Conformational Changes Combined with Charge-Transfer Interactions Are Essential for Reduction in Catalysis by p-Hydroxybenzoate Hydroxylase. *Biochemistry* **2003,** *42* (38), 11234-11242.
33. Gatti, D. L.; Palfey, B. A.; Lah, M. S.; Entsch, B.; Massey, V.; Ballou, D. P.; Ludwig, M. L., The mobile flavin of 4-OH benzoate hydroxylase. *Science* **1994,** *266*, 110-114.
34. Grzyska, P. K.; Ryle, M. J.; Monterosso, G. R.; Liu, J.; Ballou, D. P.; Hausinger, R. P., Steady-state and transient kinetic analyses of taurine/α-ketoglutarate dioxygenase: Effects of oxygen

concentration, alternative sulfonates, and active-site variants on the FeIV-oxo intermediate. *Biochemistry* **2005,** *44* (10), 3845-3855.

35. Basudhar, D.; Madrona, Y.; Kandel, S.; Lampe, J. N.; Nishida, C. R.; Ortiz de Montellano, P. R., Analysis of Cytochrome P450 CYP119 Ligand-Dependent Conformational Dynamics by Two-Dimensional NMR and X-Ray Crystallography. *J. Biol. Chem.* **2015,** *290* (16), 10000-17.

36. Daubner, S. C.; Avila, A.; Bailey, J. O.; Barrera, D.; Bermudez, J. Y.; Giles, D. H.; Khan, C. A.; Shaheen, N.; Thompson, J. W.; Vasquez, J.; Oxley, S. P.; Fitzpatrick, P. F., Mutagenesis of a specificity-determining residue in tyrosine hydroxylase establishes that the enzyme is a robust phenylalanine hydroxylase but a fragile tyrosine hydroxylase. *Biochemistry* **2013,** *52*, 1446-1455.

37. Daubner, S. C.; Melendez, J.; Fitzpatrick, P. F., Reversing the substrate specificities of phenylalanine and tyrosine hydroxylase: Aspartate 425 of tyrosine hydroxylase is essential for L-DOPA formation. *Biochemistry* **2000,** *39*, 9652-9661.

38. Francisco, W. A.; Tian, G.; Fitzpatrick, P. F.; Klinman, J. P., Oxygen-18 kinetic isotope effect studies of the tyrosine hydroxylase reaction: Evidence of rate limiting oxygen activation. *J. Am. Chem. Soc.* **1998,** *120*, 4057-4062.

39. Ansari, A.; Jones, C.; Henry, E.; Hofrichter, J.; Eaton, W., The role of solvent viscosity in the dynamics of protein conformational changes. *Science* **1992,** *256* (5065), 1796-1798.

40. Karsten, W. E.; Lai, C.-J.; Cook, P. F., Inverse solvent isotope effects in the NAD-Malic enzyme reaction are the result of the viscosity difference between D_2O and H_2O Implications for solvent isotope effect studies. *J. Am. Chem. Soc.* **1995,** *117*, 5914-5918.

41. Sobrado, P.; Fitzpatrick, P. F., Solvent and primary deuterium isotope effects show that lactate CH and OH bond cleavages are concerted in Y254F flavocytochrome b_2, consistent with a hydride transfer mechanism. *Biochemistry* **2003,** *42* (51), 15208-15214.

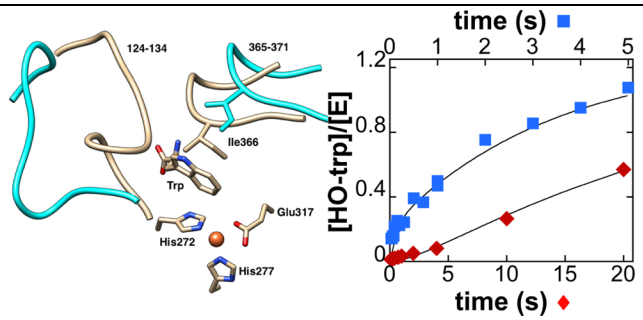
124-134
365-371
Ile366
Trp
Glu317
His272
His277
time (s)
[HO-trp]/[E]
time (s)